2016-06

Radiation effects in dual heat sinks for cooling of concentrated photovoltaics

Brandau, Mark T.

Monterey, California: Naval Postgraduate School

NAVAL POSTGRADUATE SCHOOL

MONTEREY, CALIFORNIA

THESIS

RADIATION EFFECTS IN DUAL HEAT SINKS FOR COOLING OF CONCENTRATED PHOTOVOLTAICS

by

Mark T. Brandau

June 2016

Thesis Advisor: Garth Hobson
Co-Advisor: Anthony Gannon

THIS PAGE INTENTIONALLY LEFT BLANK

REPORT DOCUMENTATION PAGE			*Form Approved OMB No. 0704–0188*

1. AGENCY USE ONLY	**2. REPORT DATE** June 2016	**3. REPORT TYPE AND DATES COVERED** Master's thesis

4. TITLE AND SUBTITLE
RADIATION EFFECTS IN DUAL HEAT SINKS FOR COOLING OF CONCENTRATED PHOTOVOLTAICS

5. FUNDING NUMBERS

6. AUTHOR(S) Mark T. Brandau

7. PERFORMING ORGANIZATION NAME(S) AND ADDRESS(ES)
Naval Postgraduate School
Monterey, CA 93943-5000

8. PERFORMING ORGANIZATION REPORT NUMBER

9. SPONSORING /MONITORING AGENCY NAME(S) AND ADDRESS(ES)
Project supported by the Office of Naval Research's (ONR) Energy Systems Technical Evaluation Program (ESTEP) supported by Dr. Richard Carlin and under the technical monitoring of Stacey Curtis.

10. SPONSORING / MONITORING AGENCY REPORT NUMBER

11. SUPPLEMENTARY NOTES The views expressed in this thesis are those of the author and do not reflect the official policy or position of the Department of Defense or the U.S. Government. IRB Protocol number ____N/A____.

12a. DISTRIBUTION / AVAILABILITY STATEMENT
Approved for public release; distribution is unlimited

12b. DISTRIBUTION CODE

13. ABSTRACT (maximum 200 words)

This thesis experimentally and numerically examined the effectiveness of improving the cooling of concentrated photovoltaics (CPV) through the use of dual heat sinks. The intent was to improve heat transfer by radiation to lower the operating temperature of the CPV system, and therefore increase the power output. Experimental and numerical results were obtained for multiple configurations to determine the effect of increased emissivity of the sink to reject heat to a ground-based sink and the effect of lowering ground temperature. Experimental results indicated that a properly constructed pin fin sink could improve heat transfer and lower operating temperature at near horizontal angles of inclination of the CPV panel. However, numerical modeling with conditions more closely matching the intended application indicates that dual heat sinks interfere with natural convection sufficiently to reduce cooling and therefore efficiency. Evaluation of these results will provide insight to improve the cooling of CPV systems and improve the power output.

14. SUBJECT TERMS heat sinks, pin-fin, thermal radiation, CPV			**15. NUMBER OF PAGES** 59
			16. PRICE CODE
17. SECURITY CLASSIFICATION OF REPORT Unclassified	**18. SECURITY CLASSIFICATION OF THIS PAGE** Unclassified	**19. SECURITY CLASSIFICATION OF ABSTRACT** Unclassified	**20. LIMITATION OF ABSTRACT** UU

NSN 7540–01-280-5500

Standard Form 298 (Rev. 2–89)
Prescribed by ANSI Std. 239–18

THIS PAGE INTENTIONALLY LEFT BLANK

Approved for public release; distribution is unlimited

RADIATION EFFECTS IN DUAL HEAT SINKS FOR COOLING OF CONCENTRATED PHOTOVOLTAICS

Mark T. Brandau
Lieutenant, United States Navy
B.S., Carnegie Mellon University, 2009

Submitted in partial fulfillment of the
requirements for the degree of

MASTER OF SCIENCE IN MECHANICAL ENGINEERING

from the

NAVAL POSTGRADUATE SCHOOL
June 2016

Approved by: Dr. Garth Hobson
Thesis Advisor

Dr. Anthony Gannon
Co-Advisor

Dr. Garth Hobson
Chair, Department of Mechanical and Aerospace Engineering

THIS PAGE INTENTIONALLY LEFT BLANK

ABSTRACT

This thesis experimentally and numerically examined the effectiveness of improving the cooling of concentrated photovoltaics (CPV) through the use of dual heat sinks. The intent was to improve heat transfer by radiation to lower the operating temperature of the CPV system, and therefore increase the power output. Experimental and numerical results were obtained for multiple configurations to determine the effect of increased emissivity of the sink to reject heat to a ground-based sink and the effect of lowering ground temperature. Experimental results indicated that a properly constructed pin fin sink could improve heat transfer and lower operating temperature at near horizontal angles of inclination of the CPV panel. However, numerical modeling with conditions more closely matching the intended application indicates that dual heat sinks interfere with natural convection sufficiently to reduce cooling and therefore efficiency. Evaluation of these results will provide insight to improve the cooling of CPV systems and improve the power output.

THIS PAGE INTENTIONALLY LEFT BLANK

TABLE OF CONTENTS

LIST OF FIGURES

THIS PAGE INTENTIONALLY LEFT BLANK

LIST OF TABLES

THIS PAGE INTENTIONALLY LEFT BLANK

LIST OF ACRONYMS AND ABBREVIATIONS

CPV	Concentrated Photovoltaic
DOD	Department of Defense
DON	Department of the Navy
NPS	Naval Postgraduate School
NREL	National Renewable Energies Laboratory
ONR	Office of Naval Research
SECNAV	Secretary of the Navy

THIS PAGE INTENTIONALLY LEFT BLANK

NOMENCLATURE

Symbols	Description	Units
A	Area	[m^2]
ΔT	Change in temperature between heater and ambient temperature	[°C]
ε	Emissivity of a material	[Dimensionless]
F_{12}	View Factor between two objects	[Dimensionless]
σ	Stephan-Boltzmann Constant	$[\frac{W}{m^2K^4}]$
θ	Angle off the horizontal of heat sink	[°]
q_{rad}	Radiative Heat Transfer	[W]
T_{amb}	Ambient Temperature	[°C]
T_c	Chiller Temperature	[°C]
T_h	Heater Temperature	[°C]
T_{sink}	Sink Temperature	[°C]

THIS PAGE INTENTIONALLY LEFT BLANK

ACKNOWLEDGMENTS

I would like to thank my advisers, Dr. Garth Hobson and Dr. Anthony Gannon, for their support and help throughout this process. Their effort and time was invaluable in making this work and getting me this far.

I would have never made it this far at Naval Postgraduate School without the support and help of my mechanical engineering classmates. Their support throughout the two years here was invaluable, and the hours they spent helping me get through this are a huge part of why I graduated. My CPV teammates helped clear the way, providing invaluable insight that helped shape my thesis.

In addition, Dr. Sanjeev Sathe was an instrumental part of this thesis and my successful graduation. He was a mentor, teacher, and friend, and the lessons I learned from him both in and out of the classroom are ones that will help me for the rest of my life.

I also would like to thank my family and friends for their support and encouragement throughout my time at NPS, and a special acknowledgment goes to Derek and Justin, who made this tour and my time in Monterey one worth remembering.

THIS PAGE INTENTIONALLY LEFT BLANK

I. INTRODUCTION

A. PROBLEM STATEMENT

Worldwide energy consumption continues to grow, with the Department of Defense as one of the greatest energy consumers in the United States. In October 2009, Secretary of the Navy (SECNAV) Ray Mabus announced a series of green energy goals for the Department of the Navy:

- **Energy efficient acquisition:** Evaluation of energy factors will be mandatory when awarding contracts for systems and buildings.
- **Sail the "Great Green Fleet":** DON will demonstrate a Green Strike Group in local operations by 2012 and sail it by 2016.
- **Reduce non-tactical petroleum use:** By 2015, DON will reduce petroleum use in the commercial vehicle fleet by 50%
- **Increase alternative energy ashore:** By 2020, DON will produce at least 50% of shore based energy requirements from alternative sources; 50% of DON installations will be net-zero
- **Increase alternative energy use DON-wide:** By 2020, 50% of total DON energy consumption will come from alternative sources[1].

In support of these goals, the Office of Naval Research (ONR) chose to investigate solar power for use at naval shore installations. In support of ONR research, this thesis will specifically examine concentrated photovoltaic (CPV) technology. CPV is noted by the National Renewable Energies Laboratory (NREL) as a young and emerging technology with the potential to overtake flat-panel photovoltaics in cost effectiveness [2]. This thesis examines means to improve concentrated photovoltaic (CPV) technology in support of SECNAV energy goals, the final two dealing with alternate energy ashore.

Solar power technology continues to evolve. CPV technology is quickly maturing, and presents unique challenges for design applications, in contrast to conventional systems. Conventional photovoltaics simply have incident solar radiation impinge on a semiconductor, CPV uses magnifying lenses to concentrate a given area of solar radiation onto a much smaller area. This permits the use of much smaller semiconductors to convert to electrical power, and thus less semiconductor material can be used to collect

the same amount of solar radiation. These advanced multi-junction semiconductors can have conversion efficiencies of nearly double those of flat-panel silicon [3]. These advanced semiconductors, however, are much more expensive on a per-area basis than single junction cells, so solar concentration is employed to minimize the area of the advanced semiconductor and reduce system cost. Figure 1 shows a concept schematic of a basic CPV system.

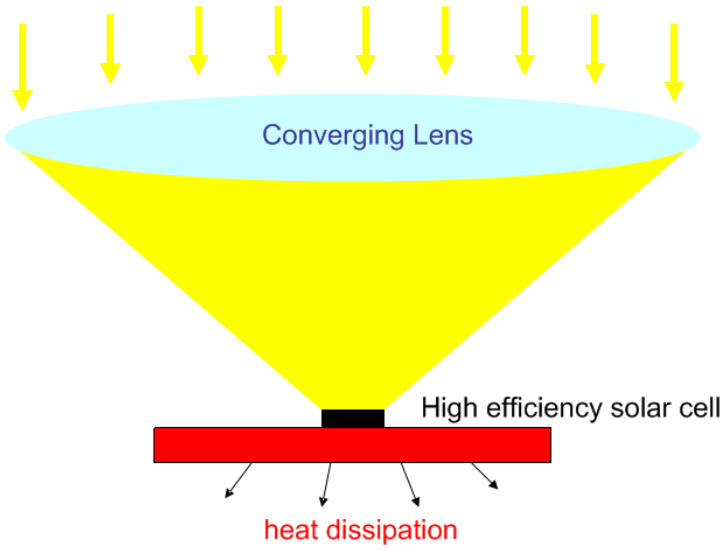

Figure 1. Schematic of a Concentrated Photovoltaic System. Source: [4]

A major drawback of solar concentration is the temperature rise inherent in concentrating solar energy onto a much smaller area. The efficiency of any solar cell decreases as semiconductor material temperature increases, and this is more pronounced with advanced multi-junction chips. Figure 2 shows several temperature-efficiency curves for several semiconductors. Cooling CPV systems is thus an issue worth examining, as a more effective cooling system results in greater energy conversion at the solar cell, and thus greater power output from a solar power plant. While the improvement may be small, in a large-scale installation with a life cycle of 15–20 years, even a small increase in efficiency of 0.1% to 0.2% can result in improved power generation and greater return on investment over the life of the plant. This factor drove the investigation into radiation as a potential low-cost means to improve cooling, and thus CPV power output.

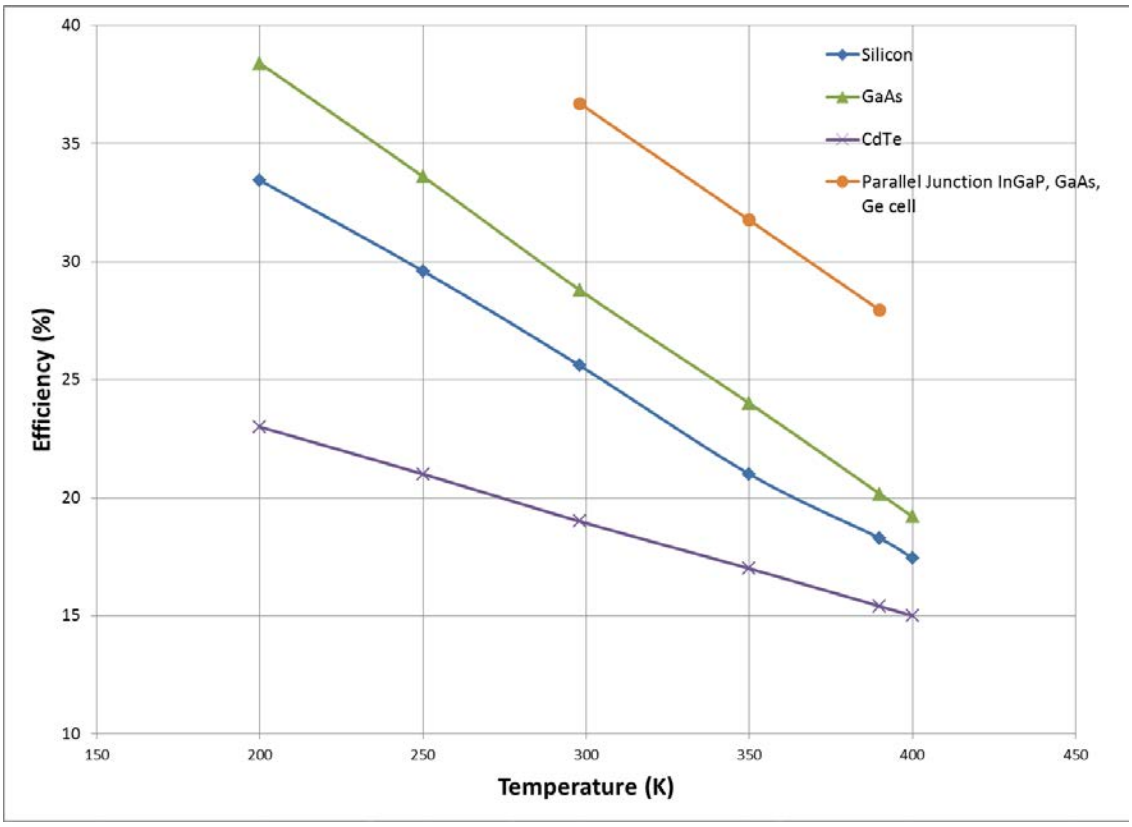

Figure 2. Temperature-Efficiency Curves of Select Solar Cells. Adapted from [5, 6]

B. GOALS

The goal of this thesis was to examine various parameters of heat sinks that would improve radiative heat transfer. For experimental results, this was accomplished by varying the angle of inclination (θ), the heat sink profile, and the temperature of the radiative heat sink (T_{sink}). These same parameters were examined in numerical results. The heat sink's angle of inclination was measured from the horizontal, with the height of the lowest point on the heater's heat sink fixed. Two different pin fin sinks were tested to examine the impact of sink height on the disruption of natural convection. An active cooling system was used to determine the effect of lowering ground temperature on overall heat transfer. The goal was to provide experimental data to determine if the improved radiation heat transfer of dual sinks outweighs the disruption to natural convection flows. To provide a broader range of testing conditions, ANSYS modeling

tested additional configurations for varying states of emissivity and conditions. The evaluation of the effect of these parameters provided insight into means to improve and optimize cooling of concentrated photovoltaics.

C. SCOPE

Based on Mai's work at the Naval Postgraduate School [7], this thesis will examine means to improve heat transfer via radiative means by providing a near-blackbody heat sink to which waste heat will be rejected via radiation. This thesis examined experimental results utilizing two different kinds of pin fin heat sinks, one low and one high profile, with the low profile sink additionally tested with active cooling. The first part of this thesis examined the results of these experiments by comparing baseline results of the heater with sink against the results of the heater sink combination with a radiative sink on the deck. This testing was conducted at multiple angles off the horizontal. The second part of this thesis examined 2-D ANSYS simulations of simple 3-pin sinks tested at multiple angles and configurations with a steady heat input to examine the effect of radiation under different conditions from those tested experimentally. The final portion was a conclusion about the effectiveness of dual pin-fin sinks to improve heat transfer in CPV technologies.

II. THEORETICAL BACKGROUND

A. CPV COOLING

The concentration process for CPV systems results in significant heat generation in the solar cell. This is detrimental to cell performance, as this temperature increase leads to reduced cell efficiency, and consequently reduced power generation. As such, the removal of heat from CPV systems is vital. Heat transfer out of a system is via conduction, convection, or radiation. While convective transfer is dominant, work done at the Naval Postgraduate School shows that a significant portion of heat transfer out of a module is by radiation [7].

1. Previous work

Previous work in field has been focused on improving convection transfer via improved heat sinks. While radiation is always accounted for on the actual module by using high emissivity substrates, the effects of improving radiative heat transfer by additional heat sinks or improved emissivity of the ground has not been studied in depth. This is due to the high natural emissivity of most surfaces where large scale CPV plants are installed. Table 1 lists the emissivities of common materials CPV plants are mounted in, along with anodized aluminum for reference.

Table 1. Emissivities of Common Materials upon Which CPV Systems Are Mounted

Heater Power Tested (W)				
Soil	Asphalt	Concrete	Sand	Aluminum
0.9	0.85	0.88	0.9	0.84

However, according to research by Mai [7], radiation accounts for nearly 40% of the heat transfer out of a pin fin heat sink. With so much energy transfer via radiative means, efforts to improve this are a logical topic to investigate. This thesis will examine means to

improve this via the use of ground-mounted pin fin heat sinks to serve as radiation sinks in order to reduce the operating temperature of CPV systems by exploiting the cavity effect.

B. THEORY

1. Radiation Modeling

Heat transfer by radiation is dependent on several factors. The radiation transfer in a two surface enclosure is defined by the Stephan-Boltzmann law and Kirchoff's law, combined in the following equation [8]:

$$q_{rad} = \frac{\sigma\left(T_1^4 - T_2^4\right)}{\frac{1-\varepsilon_1}{\varepsilon_1 A_1} + \frac{1}{A_1 F_{12}} + \frac{1-\varepsilon_2}{\varepsilon_2 A_2}} \tag{1}$$

The numerator captures the effect of temperature difference in the heat exchange. The denominator captures the effect of the emissivity of each surface and the view factor from one surface to the other. This thesis examines increasing both effective emissivity and view factors of the cold surface to improve heat transfer out of the hot surface, thus lowering the cell operating temperature.

Emissivity is defined as the ratio of radiation emitted by a real body when compared to a black body [8]. This factor means that real bodies with emissivity less than one can be improved. By raising the emissivity of a body, radiative heat transfer will improve, alternatively lowering it reduces heat transfer by radiation. The use of materials that have high emissivity can improve heat transfer, and the contrast between high and low emissivity can help as well.

View factor is the second major factor this thesis will examine. View factor is defined as "the fraction of radiation leaving surface 1 that is intercepted by surface 2." [8]. A larger or more prominent surface will increase the view factor between two surfaces according to the integral:

$$F_{12} = \frac{1}{A_1} \int_{A_1} \int_{A_2} \frac{\cos\theta_1 \cos\theta_2}{\pi R^2} dA_1 dA_2 \tag{2}$$

By increasing the value of this integral with respect to a high emissivity heat sink, additional heat can be extracted from a body via radiation. By employing finned heat

sinks to improve radiation transfer, it increases the view factor between the radiating object and the pin fin sink using the cavity effect, which is explained in more detail below. When the view factor between two objects increases, the heat transfer between them goes up. If the object whose view factor is increased also has an increased ε, then overall heat transfer out of the radiating object increases further.

Additionally, a pin fin heat sink creates the phenomenon known as the cavity effect. The cavity effect in radiation is a mechanism in which cavities cut into a reradiating surface tend towards a higher effective emissivity than their actual material. This is a result of the effective view factor into the cavity being 1, and by the relation between view factors in and out of a surface [8]

$$F_{12}A_1 = F_{21}A_2 \tag{3}$$

The effective view factor out is increased. This leads to a rise in effective emissivity to near perfect black body behavior, resulting in greater radiation absorption of a given surface with cavities compared to one without. Figure 3 illustrates the cavity effect. The cavity acts as a near perfect black body radiator even when the material emissivity is less than one.

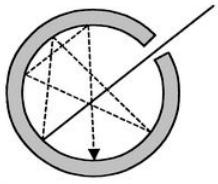

Figure 3. Blackbody Cavity Example. Source:[9]

This thesis assumed non-participating media for all calculations, as air can reasonably be assumed to be a non-participating media [8]. In participating media, the fluid that radiation is in absorbs a portion of the radiation transfer, which air does not do over short distances.

However, a side effect of employing a second finned heat sink below the photovoltaic heat sink to improve radiation transfer is that it can interfere with the natural convection heat transfer from the photovoltaic heat sink. This may result in lowering

natural convection transfer to the point of actually lowering overall heat transfer out of the heater despite the improvement in radiative transfer. This potential interference will be a primary concern of this thesis, as improved radiation transfer will not be realized if the means to improve radiation transfer reduces convective transfer by more than the gain in radiation.

III. EXPERIMENTAL METHODOLOGY

A. EXPERIMENTAL SETUP

Experiments were conducted to determine the impact of a radiation sink on a heating element across a variety of conditions. This included varying conditions of ground based sinks to examine the effect on emissivity and the effect of lowering ground temperature.

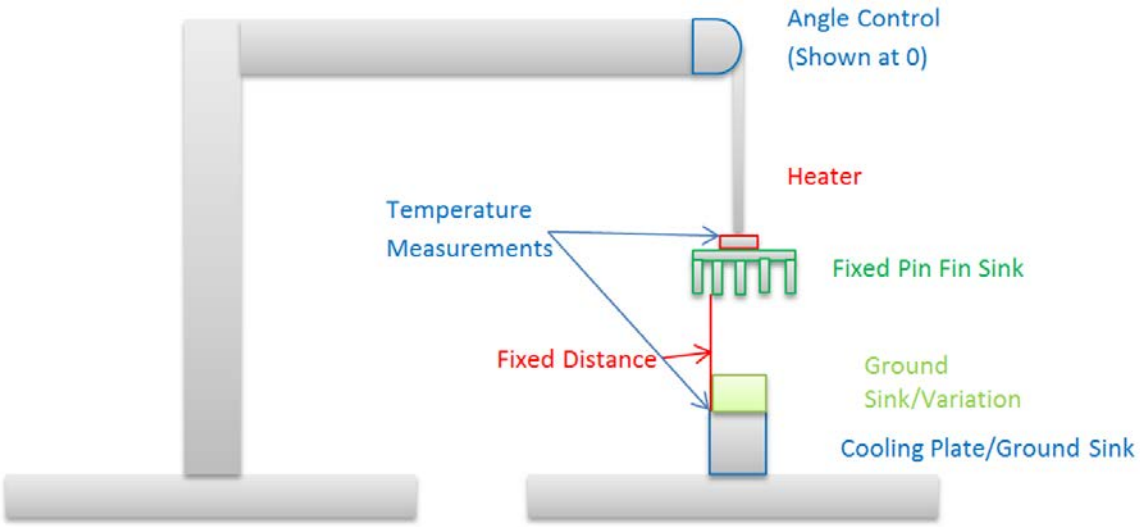

Figure 4. Schematic of Experimental Setup. Angle Control Shown at 0°

1. Experimental Equipment

This experiment utilized a WATLOW ceramic heater as the heat source for all experiments with dimensions 0.0254m X 0.0254m X 0.00254m. Two wires connected this to a BK Precision XLN15010 High Power Programmable DC Power Supply for precision power input. Diegel [10] and Mai [7] used the same heater and wire combination in their experiments, and their results show that the wire resistance is less than 1% of the heater. Mai's experiments using similar methodology also displayed valid results with this heater combination. Temperature measurements were taken on a type K thermocouple connected to a Martel Electronics PTC8010 precision measuring device.

The heating element was clamped between a metal plate and a pin fin heat sink. The plate was attached via an aluminum bar to a precision distance and angle control mechanism. This was employed to control the exact height and angle of the heater and sink combination. This was mounted over a cooling plate previously employed by Diegel in his contact resistance and thermal conductivity experiments as the control for ground temperature. The height of the lowest point of the heat sink attached to the heater was precisely maintained at 0.041275 m, with the heater centered over the cooling plate. The base where the cooling plate was mounted consisted of an unpolished aluminum, with an emissivity below 0.4.

Active cooling was provided by a Heidolph RotaChill large chilling unit previously utilized by Diegel [10] in his contact resistance experiments. Active cooling was desired to test the effect of increasing the temperature difference between the heating element and the ground based radiation sink. Temperature measurements of the cooling plate were taken utilizing thermocouples embedded in a copper plate.

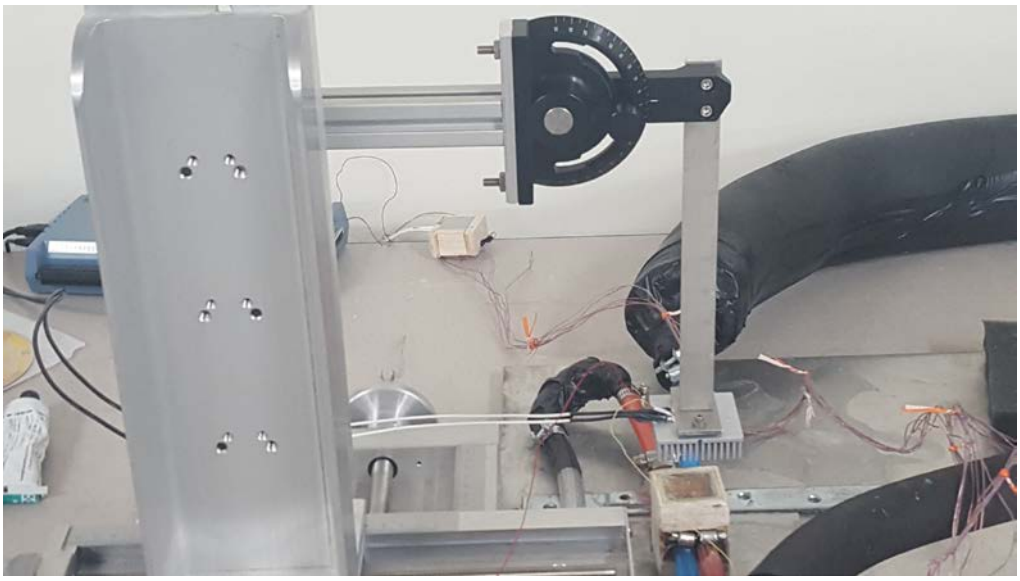

Figure 5. Experimental Setup

B. EXPERIMENTAL CONFIGURATIONS

The experiments were conducted in a lab space with ambient conditions. Prior to each experimental run, ambient temperature was measured, and it varied from 20.1°C to 23.6°C. Baseline conditions were established by an experimental run with the heater in the proper position without a ground sink in position. The baseline was tested at 14 different power settings ranging from 0.22W to 3.08W at 0°, 30°, 60°, and 90° of inclination off the horizontal.

Table 2. Heater Power Settings Tested

Heater Power Tested (W)													
0.22	0.32	0.42	0.58	0.77	0.94	1.15	1.34	1.54	1.83	2.11	2.41	2.76	3.08

At each power setting, the heater was allowed to reach steady state, which took approximately twenty minutes per setting. Power was then increased to the next measurement step once no changes over several minutes had been observed.

1. Variations Tested

With the baseline established, low profile and high profile heat sinks were then positioned directly beneath the heater-sink combination to test the effect of a passive radiation sink. The experiment was then run with the cooling system active with no ground sink to establish the effect of ground temperature, and then run again with the cooling system active and the low profile heat sink attached to test the effect of a radiative sink with cooling. For active cooling runs, the chiller temperature was set to 10°C. Steady state temperature and power were recorded across all 14 power settings for each configuration of sinks at each different angle tested. Table 3 lists the characteristics of the heat sinks tested in these experiments. Figures 6 and 7 show the radiative heat sinks and the heating element with fixed heat sink, respectively.

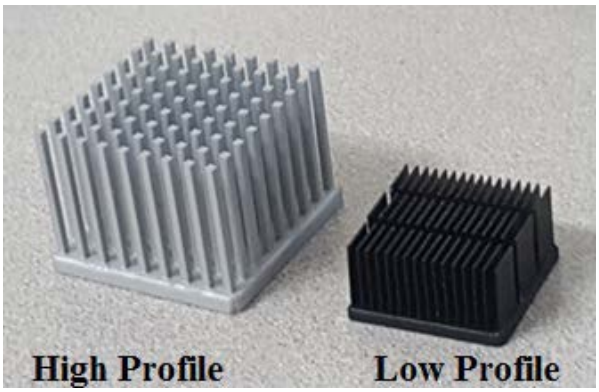

Figure 6. Radiative Heat Sinks

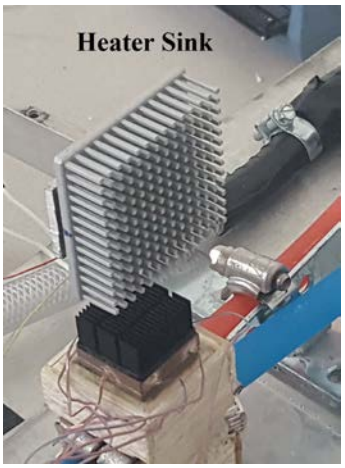

Figure 7. Heater with Sink at θ=90°

Table 3. Characteristics of Heat Sinks Tested. Source: [7]

Type	Material	Dimensions (mm)			A_s=Surface Area (mm^2)	$Volume_{solid}(mm^3)$	$\frac{A_s \text{ of heat sink}}{A_s \text{ of heater}}$
Heater Sink (196 square-pin fins)	Anodized Aluminum	1 fin	Length=	1.39±0.05	18,677±541	12,187	12.3
			Width=	1.43±0.05			
			Height=	11.89±0.05			
		Base	Length=	49.61±0.05			
			Width=	49.61±0.05			
			Height=	3.07±0.05			
High Profile (81 square-pin fins)	Anodized Aluminum	1 fin	Length=	1.35±0.05	12,535±399	6,913	8.3
			Width=	1.38±0.05			
			Height=	21.98±0.05			
		Base	Length=	34.66±0.05			
			Width=	34.71±0.05			
			Height=	2.99±0.05			
Low Profile (48 fins)	Black Anodized Aluminum	1 fin	Length=	6.4	7,496	1,430	5.0
			Width=	0.1			
			Height=	10.72			
		Base	Length=	25.03			
			Width=	25			
			Height=	1.76			

IV. EXPERIMENTAL RESULTS

A. RESULTS

For all configurations, heater temperature was recorded at each heater power. Ambient temperature was subtracted from this to compute the change in temperature, and this change in temperature was then plotted against heater power. Figures 8–11 and Tables 4–7 show the difference between heater temperature and ambient temperature against heater power in graphical and table form.

1. Plots of Experimental Results

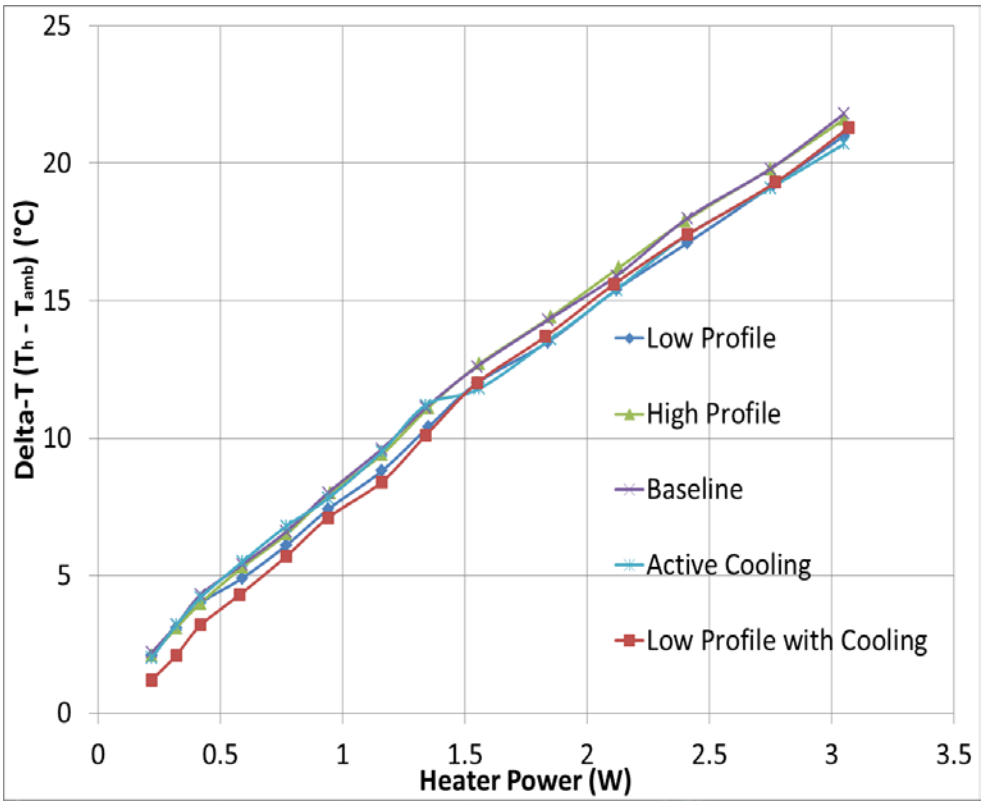

Figure 8. Plot of Change in Heater Temperature at 0° Orientation

Table 4. Summary of Change in Heater Temperature for 3.08W at 0° Orientation

Steady State ΔT at 0°					
Power	Baseline	Low Profile	High Profile	Cooling	Low profile w/Cooling
0.22	2.2	2.1	2.1	2	1.2
0.32	3.2	3.1	3.1	3.2	2.1
0.42	4.3	4	4	4.2	3.2
0.59	5.4	4.9	5.3	5.5	4.3
0.77	6.6	6.1	6.5	6.8	5.7
0.94	8	7.4	8	7.8	7.1
1.16	9.6	8.8	9.4	9.5	8.4
1.34	11.1	10.4	11.1	11.2	10.1
1.55	12.6	12	12.7	11.8	12
1.84	14.3	13.5	14.4	13.6	13.7
2.12	15.9	15.4	16.2	15.4	15.6
2.41	18	17.1	17.9	17.4	17.4
2.75	19.8	19.2	19.8	19.1	19.3
3.05	21.8	21	21.6	20.7	21.3

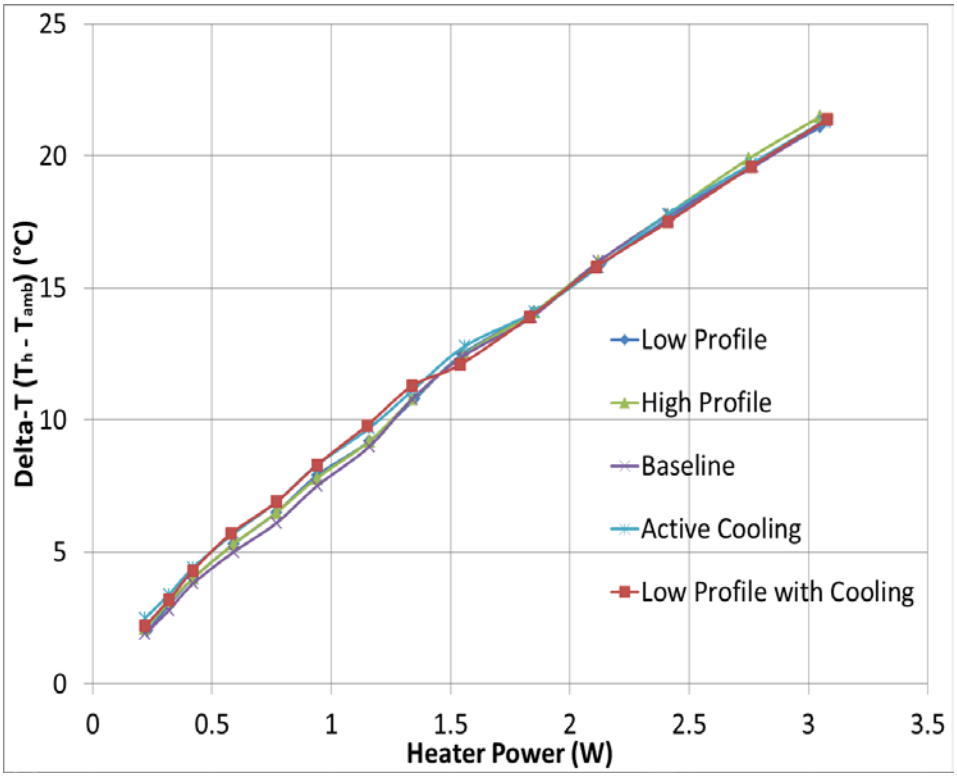

Figure 9. Plot of Change in Heater Temperature at 30° Orientation

Table 5. Summary of Change in Heater Temperature for 3.08W at 30° Orientation

Steady State ΔT at 30°					
Power	Baseline	Low Profile	High Profile	Cooling	Low profile w/Cooling
0.22	1.9	2	2.1	2.5	2.2
0.32	2.8	3	3.1	3.4	3.2
0.42	3.8	4	4	4.4	4.3
0.59	5	5.3	5.3	5.7	5.7
0.77	6.1	6.5	6.5	6.9	6.9
0.94	7.5	7.9	7.8	8.3	8.3
1.16	9	9.2	9.2	9.7	9.8
1.34	10.8	10.8	10.8	11.2	11.3
1.55	12.4	12.5	12.5	12.8	12.1
1.84	13.9	14.1	14.1	14.1	13.9
2.12	16	15.9	16	15.8	15.8
2.41	17.8	17.6	17.8	17.8	17.5
2.75	19.6	19.6	19.9	19.7	19.6
3.05	21.3	21.1	21.5	21.3	21.4

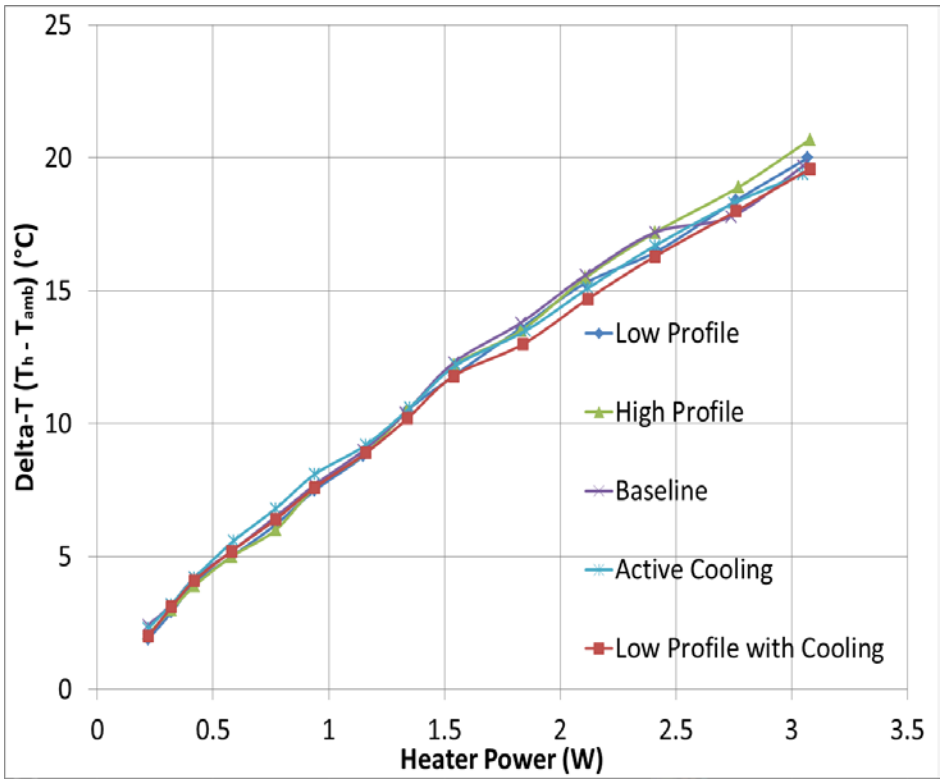

Figure 10. Plot of Change in Heater Temperature at 60° Orientation

Table 6. Summary of Change in Heater Temperature for 3.08W at 60° Orientation

Steady State ΔT at 60°					
Power	Baseline	Low Profile	High Profile	Cooling	Low profile w/Cooling
0.22	2.4	1.9	2.1	2.3	2
0.32	3.2	2.9	3	3.2	3.1
0.42	4.2	4	3.9	4.2	4.1
0.59	5.2	5	5	5.6	5.2
0.77	6.5	6.2	6	6.8	6.4
0.94	7.7	7.5	7.6	8.1	7.6
1.16	9	8.8	8.9	9.2	8.9
1.34	10.4	10.5	10.5	10.6	10.2
1.55	12.3	11.8	12.2	12.2	11.8
1.84	13.8	13.6	13.5	13.5	13
2.12	15.6	15.3	15.5	15.1	14.7
2.41	17.2	16.5	17.2	16.7	16.3
2.75	17.8	18.4	18.9	18.3	18
3.05	19.7	20	20.7	19.4	19.6

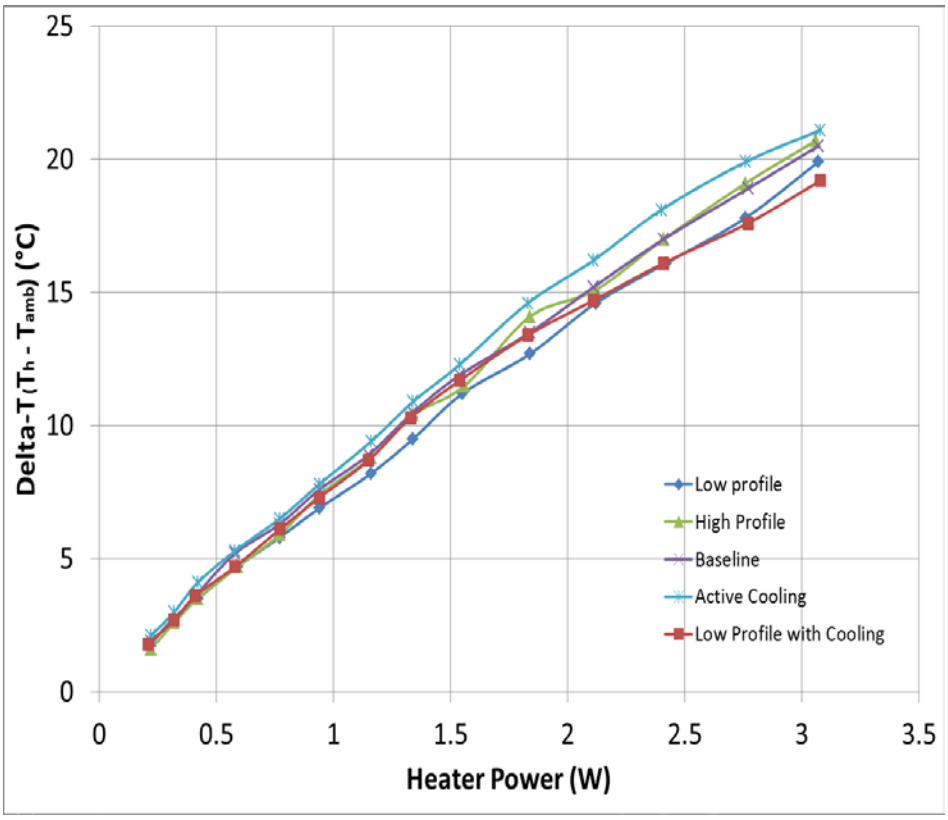

Figure 11. Plot of Change in Heater Temperature at 90° Orientation.

Table 7. Comparison of Change in Heater Temperature at 90° Orientation

Steady State ΔT at 90°					
Power	Baseline	Low Profile	High Profile	Cooling	Low profile w/Cooling
0.22	1.9	1.8	1.6	2.1	1.8
0.32	2.7	2.8	2.6	3	2.7
0.42	3.7	3.5	3.5	4.1	3.6
0.59	5.2	4.7	4.7	5.3	4.7
0.77	6.3	5.8	5.9	6.5	6.1
0.94	7.6	6.9	7.4	7.8	7.3
1.16	8.9	8.2	8.8	9.4	8.7
1.34	10.5	9.5	10.4	10.9	10.3
1.55	11.9	11.2	11.5	12.3	11.7
1.84	13.5	12.7	14.1	14.6	13.4
2.12	15.2	14.6	15.1	16.2	14.7
2.41	17	16.1	17	18.1	16.1
2.75	18.9	17.8	19.1	19.9	17.6
3.05	20.5	19.9	20.7	21.1	19.2

B. ANALYSIS OF EXPERIMENTAL RESULTS

1. Effect of Ground-Mounted Heat Sinks and Active Cooling

a. 0° Inclination

The addition of the low and high profile heat sinks showed varying results. When compared to the baseline case at 0° inclination, there was a clear improvement with both the low and high profile sinks at 0° inclination. At 0°, research by Mai showed that natural convection was effectively suppressed with pin fin sinks [7], thus the improved radiation sink provided by the ground mounted pin fin sinks provided a clear improvement on heat transfer, with 0.8°C improved cooling provided by the low profile sink at maximum power input. Even the high profile sink provided improved cooling at 0° inclination. This shows that the ground based sinks can be effective at this inclination.

Active Cooling at this angle showed the greatest impact it will have, lowering the operating temperature by over a degree for the simple cooling and 0.4°C for the low profile sink with cooling at maximum power. This shows that the increased temperature differential between the heater and the base at high power showed dramatically increased cooling, which would lead to potentially a full 0.2% increase in efficiency of a solar cell.

b. 30° Inclination

However, at 30° inclination the first break over occurs. Natural convection is no longer suppressed at this angle, and as such, the baseline shows improved cooling. While the low profile sink still showed better cooling than the baseline case by 0.2°C, the high profile sink shows worse cooling by 0.2°C. This is due to interference with natural convection by that high profile sink, a phenomenon that will be demonstrated numerically. This increase in natural convection cooling for the baseline agrees with Mai's research [7], providing additional validation of the experiment.

The cooling system shows very little effect at this angle. The base cooling effect shows zero change from the baseline condition, while the low profile with cooling shows a 0.1°C increase in temperature. This massive degradation of cooling is a result of natural convection taking over and becoming dominant, vastly lessening the effect the improved radiation when compared to the 0° inclination case.

c. 60° Inclination

At 60°, a breakdown is seen. Both the low and high profile sink provide inferior cooling to the baseline at this angle. This shows a surprising disparity with other results, but is a result of natural convection achieving dominance at this angle and the improved radiation effects of the ground sinks being offset by their suppression of convection transfer. 60° is a critical angle for this, as natural convection is not yet maximized, but the impact of the sinks on it interferes with natural convection by the greatest margin, as the 90° tests do not match this.

The effects of cooling on the 60° trials closely matched the 30°. While both cooling and low profile with cooling showed improved operating temperature, the difference in each case at maximum power was minimal.

d. 90° Inclination

At 90°, the low profile sink crossed over and regained its effectiveness. This is due to the 90° inclination having the greatest natural convection transfer as a result of the geometry and surface area on which convection occurs. This results in the suppression

effect of the low profile ground sink, while still occurring, not degrading convection to the point where it loses effectiveness, and cooling the heater by an additional 0.6°C. However, the high profile ground sink continues its trend of being less effective, and ends up degrading cooling to the effect of a 0.2°C increase in operating temperature.

At 90°, the cooling trials showed very interesting results. The basic cooling showed an increase in operating temperature by 0.6°C, while the low profile with cooling generated 1.3°C in operating temperature decrease at full power.

2. Disparity with Real-World Conditions

Of note, these trials were conducted at conditions not matching anticipated real world conditions. The large aluminum plate the entire experimental setup was mounted over has a much lower emissivity than the surfaces on which major power plants of CPV systems would be mounted. To test that, numerical models were run with conditions approximating real world.

THIS PAGE INTENTIONALLY LEFT BLANK

V. NUMERICAL METHODOLOGY

A. ANSYS SOFTWARE

The ANSYS software's CFX computational fluid dynamics module was employed to numerically model the effect of simplified pin fin heat sinks on heat transfer in a two dimensional domain. ANSYS software is industry standard software for CFD work and accurately models fluid flow and heat transfer over a wide variety of conditions. It was employed to numerically model the effect of pin fin heat sinks on heat transfer over conditions closely matching intended use of CPV plants when compared to the experimental models.

B. SOFTWARE SETUP

1. Physical Models

ANSYS settings were run as a single domain. All geometries were imported as parasolid solid models after being generated in the solid modeling program Solidworks. For this, the heat sink was simplified to a 3-pin sink with fins. The base of the sink was 0.03175m X 0.00635m X 0.00635m, with fins of 0.00635 X 0.003175 X 0.03175m extending from it with 0.00635m of separation between fins. The fins long base edge was flush with the edge of the fluid domain. This sink was inserted as a cavity into a fluid domain at a prescribed angle, and then either a duplicate sink or a sink with fins 1/3 the length was inserted into a cavity at the base of the fluid domain as a second cavity. Figures 12 and 13 show the heat sinks and an example of the fluid domain tested, respectively.

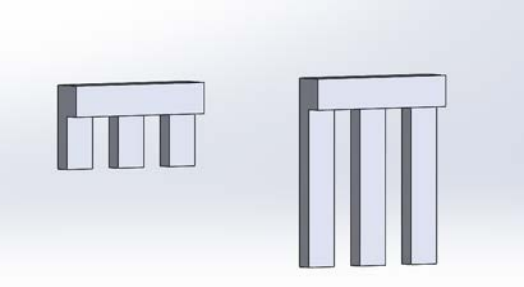

Figure 12. Solidworks Generated 3-Pin Heat Sinks—Low and High Profile

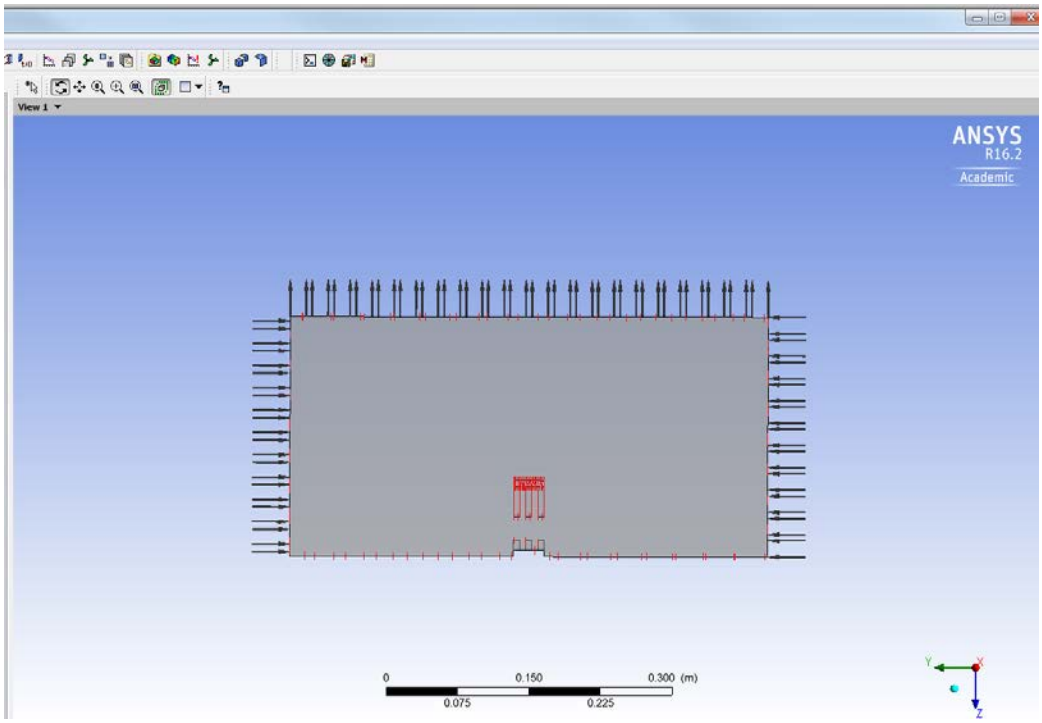

Figure 13. Example ANSYS Domain

2. Meshing

With models constructed, the meshing was the next major step. With the only area of concern being that immediately around the heat sink and heater, edge sizing of 0.0005m was employed on all edges of the heater and heat sink. This created a very fine mesh in the area of concern for natural convection while leaving the mesh coarse outside the area of concern, optimizing the computation time for a given mesh while providing sufficient accuracy to provide valid data.

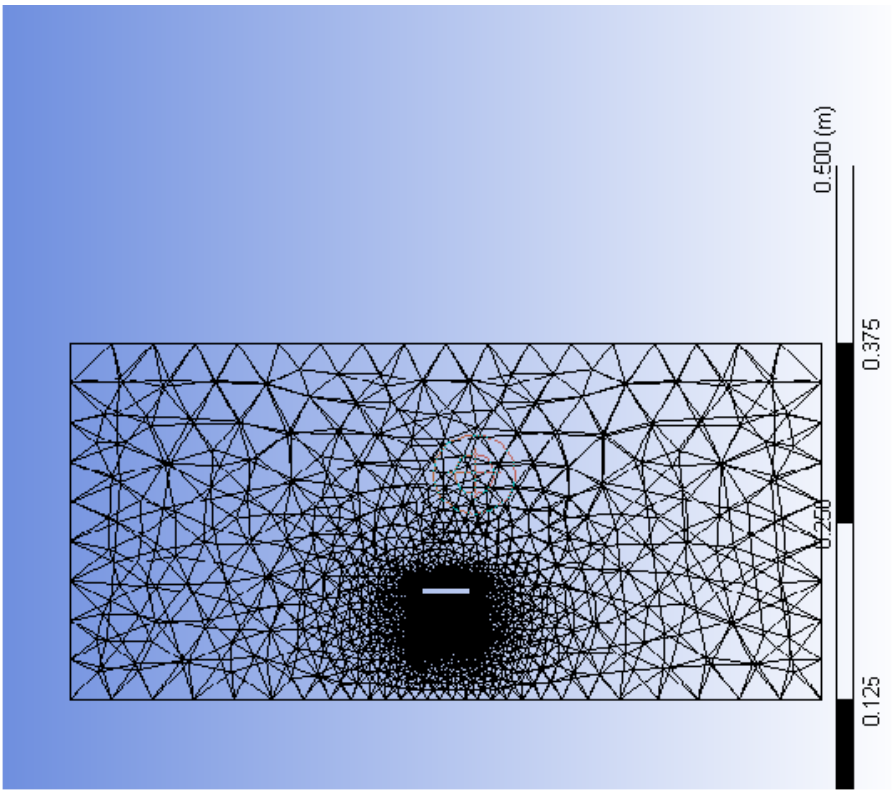

Figure 14. Example ANSYS Mesh

3. Boundary Conditions

The meshed model was loaded into CFX-Pre to establish boundary conditions. The fluid domain was modeled as “Air Ideal Gas” with turbulence modeling set to laminar flow. Initial runs were conducted as steady state simulations, with total energy involved over the domain. Domain initialization was used to set the velocity to 0 m/s in all three axis directions with no pressure gradient. The heating element was modeled as a wall with a constant heat flux of 400 W/m^2 to simulate the heat input of the heating element. The floor of the simulation, modeling the ground, was modeled as a constant-temperature wall. The sides of the domain were modeled as inlets with a relative stagnation pressure of 0 Pa. The top of the simulation was modeled as an outlet with a relative static pressure of 0 Pa. The large sides were treated as a Symmetry boundary condition to keep the model as a two dimensional one. When inserted, the ground-based heat sink was also modeled as a constant temperature wall. See Figure 13 for a view of

the basic model. This model was run first to establish that heat transfer occurred, and then buoyancy was added to account for natural convective transfer.

4. Natural Convection Modeling

With the basic model validated, the buoyancy setting was enabled to allow for natural convection. Buoyancy is the driving force in the CFX module to create natural convection flow. Once buoyant flow is introduced to the simulation, gravity and reference density settings are required. Gravity was set in the negative Z direction at 9.81 m/s^2. Reference density was set at 0. With these settings, the model was run to establish good natural convection flow. This was established, and the good streamlines and vector plot of velocity were used to validate the model's convection flow. See Figure 15 for a screen capture of convective flow.

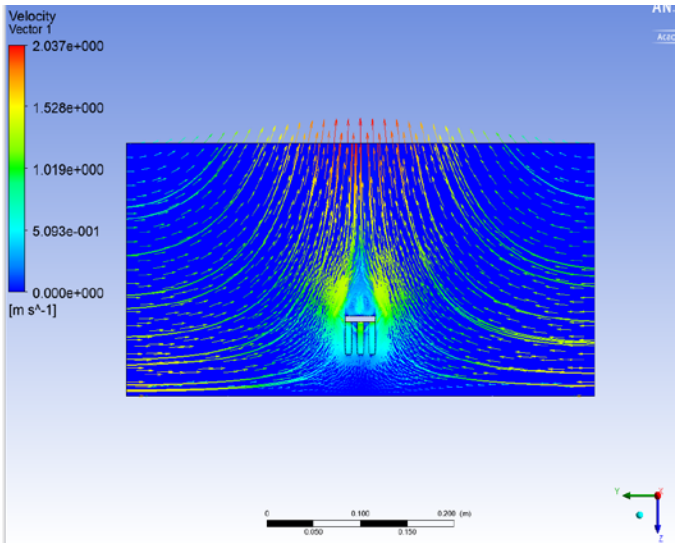

Figure 15. ANSYS Screen Capture of Natural Convection in 0° Baseline Case

5. Radiation Modeling

With natural convection flow validated in the model, the final addition to the model was to include radiation. ANSYS offers four different methods to compute radiation heat transfer. For this thesis, the Discrete Transfer method was employed. This is the most accurate method offered, where each element employs multiple rays traced

out of it. The default ray setting is 8 rays, this thesis employed models varying from 20 to 25 rays in most models. A run with 40 rays was conducted and determined to have less than a 0.2% effect on maximum temperature. Modeling was conducted using the Surface-to-Surface option, assuming air was a non-participating media and therefore neglecting the effect of air's transmissivity on radiation. For the openings at the sides and top of the model, an external blackbody temperature of 21°C was selected for radiation at the boundary, approximating real-world conditions at that temperature.

Emissivity settings for the heater and deck sink were treated as black anodized aluminum, with a value of 0.88. For the floor, the emissivity of asphalt from Table 1 was employed [8]. The simulations run with radiation enabled showed greater heat transfer and lower heater temperature than the pure convection model, and thus provided a fully validated model.

6. Variations Tested

Once a valid model and boundary conditions had been established for the baseline simulation, variations were introduced and tested. The geometry of the model was altered, with the heater tested at 0°, 30°, 60° and 90° off the horizontal. Additionally, the heater was tested with no ground-based radiation sink, the low profile ground sink, and the high profile ground sink at the ambient temperature of 21°C. To simulate the cooling system employed in experimental results, additional trials with the low profile sink were conducted with the constant wall temperature of the ground sink set at 10°C.

In addition to testing all four configurations at all four geometries, additional simulations were conducted. Transient modeling was conducted utilizing a total time of 2s and a timestep of 0.005s in order to determine if the simulation was unsteady. A run with a ray count of 40 for radiation transfer was to test the impact of emissivity difference between the ground based sink and the environment, simulations with the ground emissivity set at 0.2, 0.4, and 0.6 were conducted both with no ground sink and with the low profile sink present.

Table 8. Simulations Run

Simulations Run								
Angle (°)	Baseline Steady	Baseline Transient	Low Profile High Ray Count	Low Profile Steady	Low Profile Unsteady	Low Profile Cooling Steady	Low Profile Cooling Unsteady	High Profile Steady
0	X	X	X	X	X	X	X	X
30	X	x		X	X	X		X
60	X	x		X		X	X	
90	X			X		X		

VI. NUMERICAL RESULTS

A. ANALYSIS OF NEAR REAL-WORLD CONDITIONS CASES

1. Basic Settings

The basic models run with an emissivity on the ground of 0.85 and with an emissivity of the heater and ground sink of 0.88 showed data quite different from experimental. However, with the high natural emissivity of the ground in these simulations, and the degradation to convective transfer, produced predictable results in the basic simulations tabulated below.

Table 9. Summary of Numerical Maximum T_h

Inclination: 0 Degrees		Inclination: 30 Degrees		Inclination: 60 Degrees		Inclination: 90 Degrees	
Configuration	T_{max} (°C)	Configuration	T_{max} (°C)	Configuration	T_{max} (°C)	Configuration	T_{max} (°C)
Baseline	77.25	Baseline	56.05	Baseline	64.65	Baseline	32.95
Low Profile	79.65	Low Profile	69.05	Low Profile	68.858	Low Profile	37.85
Low Profile High Ray Count	80.15	High Profile	70.25	Low Unsteady	61.55	High Profile	45.85
High Profile	80.95	Low Profile w/Chiller	68.85	Low Chiller Unsteady	61.45	Low Profile w/Chiller	37.95
Low Profile w/Chiller	78.25	Baseline Unsteady	55.85	Low Profile w/Chiller	61.45		
Blackbody Deck Sink	79.75			Baseline Unsteady	63.55		
Low Profile Unsteady	84.05						
Baseline Unsteady	84.05						

In all cases except the 60° case, the same trends are captured among the numerical data. For the 0°, 30°, and 90° trials, the baseline configuration, without any ground mounted sink, provides the greatest cooling for the same heat input to the heater. Indeed, as seen in Table 9, the inclusion of the ground based sinks significantly increases operating temperature of the heater, and lowers overall heat transfer. This interference with natural convection is displayed visually below in Figure 16.

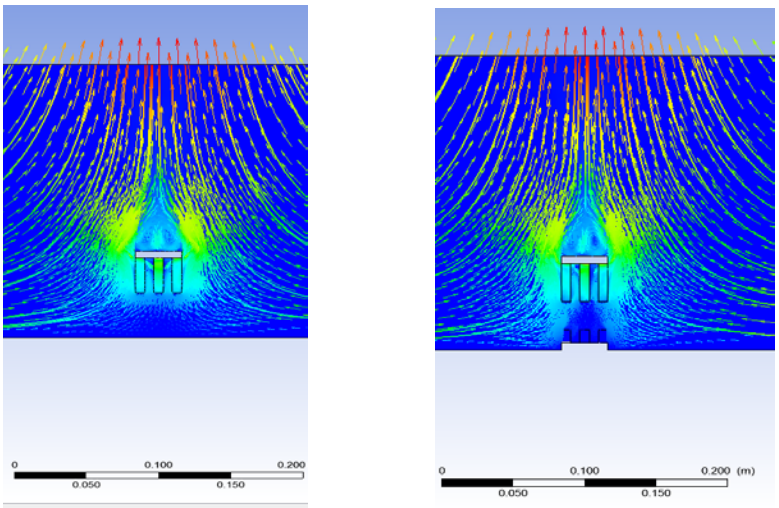

Figure 16. Comparison of Convection Flows in Baseline and Low Profile Cases

Examining Figure 16, the close up views of the areas immediately below the heat sink show that the ground sink is clearly interfering with natural convection transfer when compared to the baseline case. The lack of vector lines in and around the sink shows the lost heat transfer when compared, and the corresponding loss of heat transfer leads to the increased operating temperature of the heater. This shows that the ground sink reduces effectiveness compared to baseline, which tracks with the expectation of such a low emissivity difference, even with the cavity effect.

The 60° trials showed a slight improvement in effectiveness of cooling by the ground sinks. This is quite curious, as the experimental models also had the 60° case as the deviant from the common trend line. In the case of experimental modeling, the 60° case shows a slight improvement of cooling with the ground sinks when compared to the baseline case. For the numerical results, the 60° trials do not follow the trend of the remainder by showing slightly improved cooling for the ground sinks. This inclination bucking the trend helps validate the experimental model

2. Effect of Modeling Steady State vs Transient Fluid Flow

Baseline configuration cases were all run in both steady state and transient and in several cases transient runs were conducted other than baseline. For 0° of inclination, the unsteady case showed a 6.8°C increase in operating temperature for the baseline.

However, when run as low profile with chiller in the same unsteady condition, there was no improved cooling even in the theoretical best-case for radiation cooling to be improved. At 30°, there was no such discrepancy between transient and steady-state trials, with both cases being nearly identical in temperature readings. For the 60° case, the discrepancy was there but much lower in scope. This allowed the conclusion that regardless of transient or steady-state trials, the trend lines hold up, providing additional numerical model validation.

3. Effect of Increasing Ray Count in Discrete Transfer Radiation

To examine the effect of ray count, the Low Profile model was run at 0° with counts of 25 and 40. There was a 0.1% difference between the two cases, with the net effect being a half degree of temperature rise when the ray count was raised. This shows that the difference between the two is negligible, and all remaining cases were run with the 25 ray count setting for the Discrete Transfer model.

B. ANALYSIS OF LOW EMISSIVITY CASES

Table 10. Low Emissivity Trials Maximum Temperatures

Emissivity of Ground, Inclination = 0, ε=0.88 for Low Profile	
Model	T_{max} (°C)
ε=0.2 Low Profile	81.15
ε=0.2 Baseline	78.05
ε=0.4 Low Profile	80.55
ε=0.4 Baseline	77.95
ε=0.6 Low Profile	80.65
ε=0.6 Baseline	77.85
ε=0.85 Low Profile	79.65
ε=0.85 Baseline	77.25

In order to examine the effect of the difference in emissivity seen in the experimental results, runs were conducted varying the ground emissivity while holding the emissivity of the heater and ground sink constant at 0.88. These results are tabulated in Table 9. In each case, the trend of the low profile sink's negative impact on T_h held. The addition of a sink always lowers overall heat transfer, regardless of the emissivity of the ground. Additionally, lowering the ground emissivity reduced the heat transfer out of the heater, raising the maximum operating temperature and lowering efficiency of the CPV system. These results highlight the ineffective nature of the ground sink during numerical trials. Even with a radically higher ground emissivity to work against, the interference with natural convection these generate is simply too high to make a ground sink practicable.

C. ANALYSIS OF SPECIFIC DATA EXTRACTION

Using the ANSYS software, specific values can be extracted for heat flux values at a given surface. These are tabulated below for the four different angles. All data extracted was taken using the 'average' option in CFD Post. Radiation Flux listed is the 'Wall Incident Radiation Flux' option in CFD Posta Convection is the 'Wall Convective Heat Flux' option in CFD Post.

Table 11. Numerical Heat Fluxes for 0°

Comparison of Average Wall Fluxes [W m^-2] - 0° Inclination			
Configuration	Radiative Flux - Floor	Radiative Flux - Deck Sink	Convective Flux - Heater
Baseline	439.421	N/A	333.252
Low Profile	367	380.694	351.182
High Profile	364.998	379.096	349.634
Low Profile with Cooling	353.6	358.2	350.339

Table 12. Numerical Heat Fluxes for 30°

Comparison of Average Wall Fluxes [W m^-2] - 30° Inclination			
Configuration	Radiative Flux - Floor	Radiative Flux - Deck Sink	Convective Flux - Heater
Baseline	367.552	N/A	364.244
Low Profile	365.787	376.42	362.768
High Profile	362.787	362.787	362.787
Low Profile with Cooling	352.503	354.401	361.482

Table 13. Numerical Heat Fluxes for 60°

Comparison of Average Wall Fluxes [W m^-2] - 60° Inclination			
Configuration	Radiative Flux - Floor	Radiative Flux - Deck Sink	Convective Flux - Heater
Baseline	367.743	N/A	361.375
Low Profile	334.538	361.848	348.401
Low Profile with Cooling	321.425	339.988	346.776

Table 14. Numerical Heat Fluxes for 90°

Comparison of Average Wall Fluxes [W m^-2] - 90° Inclination			
Configuration	Radiative Flux - Floor	Radiative Flux - Deck Sink	Convective Flux - Heater
Baseline	363.183	N/A	385.812
Low Profile	363.264	372.486	385.894
Low Profile with Cooling	359.929	351.541	383.731

In every case, comparing the average absorbed radiation flux of the Floor at Baseline shows a loss of average value. Aside from the 0° case, the inclusion of a deck sink also lowers the convective flux out of the heater in each instance. However, the deck sinks add to the total surface area to absorb radiation, as tabulated below.

Table 15. ANSYS Computed Surface Area of Deck Sink and Floor for Tested Geometries

Configuration	Floor Area (m^2)	Deck Sink Area (m^2)	Area Deck Sink/Area Floor	Total Area (m^2)	%Surface Area Increase
Baseline	0.003175	0	0	0.003175	N/A
Low Profile	0.00297339	0.000685482	0.23053888	0.003658872	15.24006299
High Profile	0.00297339	0.00149193	0.501760617	0.00446532	40.64

With these areas listed, the average flux was multiplied by the surface area it impinged on to determine the net effects on radiation heat transfer, listed below in Tables 16–19.

Table 16. Comparison of Total Radiative Heat Transfer at 0°

Comparison of Total Radiation Fluxes [W] - 0° Inclination			
Configuration	Radiative Flux - Floor	Radiative Flux - Deck Sink	Total Radiative Flux
Baseline	1.395161675	N/A	1.395161675
Low Profile	1.09123413	0.260958885	1.352193015
High Profile	1.085281403	0.565584695	1.650866099
Low Profile with Cooling	1.051390704	0.245539652	1.296930356

Table 17. Comparison of Total Radiative Heat Transfer at 30°

Comparison of Total Radiation Fluxes [W] - 30° Inclination			
Configuration	Radiative Flux - Floor	Radiative Flux - Deck Sink	Total Radiative Flux
Baseline	1.1669776	0	1.1669776
Low Profile	1.087627408	0.258029134	1.345656542
High Profile	1.078707238	0.541252809	1.619960047
Low Profile with Cooling	1.048128895	0.242935506	1.291064401

Table 18. Comparison of Total Radiative Heat Transfer at 60°

Comparison of Total Radiation Fluxes [W] - 60° Inclination			
Configuration	Radiative Flux - Floor	Radiative Flux - Deck Sink	Total Radiative Flux
Baseline	1.167584025	0	1.167584025
Low Profile	0.994711944	0.248040291	1.242752235
Low Profile with Cooling	0.955721881	0.233055654	1.188777535

Table 19. Comparison of Total Radiative Heat Transfer at 90°

Comparison of Total Radiation Fluxes [W] - 90° Inclination			
Configuration	Radiative Flux - Floor	Radiative Flux - Deck Sink	Total Radiative Flux
Baseline	1.153106025	0	1.153106025
Low Profile	1.080125545	0.255332448	1.335457993
Low Profile with Cooling	1.070209289	0.240975028	1.311184317

Examining Tables 16–19, certain trends are depicted. At 0° inclination, the low profile sinks actually degrade total orientation radiation transfer out of the heater. The high profile sink, however, offers great improvement in radiation transfer. This is unfortunately offset by the massive degradation in convective transfer witnessed by the increased T_h observed in the high profile case, shown in Table 9.

However, the low profile sinks improve radiation transfer in the remaining 3 angles tested all show improved radiation transfer out of the heating element. The high

profile sink continues to show greater absorbed radiation due to its greater area; however, the massive interference this offers to natural convection in both experimental and numerical results rendered this impractical.

These increases in absorbed radiation are due to a combination of the increased surface area for transfer, which cause a higher View Factor between the heater and the deck sink. The higher view factor with the deck sink's higher emissivity material already causes theoretically improved radiation transfer. When coupled with the cavity effect raising the effective emissivity of the deck sink, we see the greater radiation transfer out of all sinks at inclinations of 30° and above, providing validation of the concept to improve radiation heat transfer.

THIS PAGE INTENTIONALLY LEFT BLANK

VII. CONCLUSION AND RECOMMENDATION

A. CONCLUSION

This thesis examined means to improve heat transfer out of a CPV module by increasing radiation cooling with attention to the natural convection out of a module. The tight confines mandated by CPV technology dictate the geometry employed, and the desire for a system with a minimal budget and no added weight to the CPV module made radiation attractive to examine. Sink profile and angle of inclination were the two variables examined by this thesis. Experimentally, it appeared that radiation sinks could in fact improve the cooling of a CPV system. However, when examined numerically, with conditions more closely matching real world conditions, the net effect was that of reduced cooling of a module due to the interference with natural convection transfer caused by the ground-mounted sinks. Even though numerical analysis showed an increase in overall radiative heat transferred, the loss of convection these sinks incurred was sufficient to render the improved radiation transfer moot.

Based on these findings, while radiation remains an important part of CPV cooling, the use of dual sinks to improve cooling is not recommended. There may be other means to improve radiation cooling of high concentration CPV systems, as their high operating temperature compared to ambient conditions leaves radiation heat transfer as a large part of their overall heat transfer.

B. FUTURE WORK

The following are potential areas with future work to improve the cooling of CPV systems through enhanced radiation transfer:

- Ground mounted heat sinks show improved radiation capture, however they degrade natural convection too greatly to be practicable. A potential project would be to design a new heat sink that retains the enhanced radiation capture of the pin fin sinks tested without interfering with natural convection.
- The effects of ground cooling showed improved transfer in all cases. Finding a means to provide ground based cooling with a minimal energy impact to the overall system would be a second area of potential research.

THIS PAGE INTENTIONALLY LEFT BLANK

LIST OF REFERENCES

[1] R. Mabus, Department of the Navy's Energy Program for Security and Independence Darby, PA: DIANE Publishing, 2010.

[2] Phillips, S. P., Bett, A.W, Horowitz, K., and Kurtz, S., 2016, "Current Status of Concentrator Photovoltaic (CPV) technology," Fraunhofer ISE/NREL, Tech. Rep. TP-6A20-63916, pp 6–10.

[3] 2016, "Best Research Cell Efficiencies," National Renewable Energies Laboratory, Rev 04–20-2016, pp.1.

[4] Liang, D., 2010, "Concentrated Photovoltaics" Stanford, large.stanford.edu/courses/2010/ph240/liang2/.

[5] Alharbi, F. H., Bousselham, A. and Hossain, M.I., 2013 "Numerical Analysis of the Temperature Effects on Single Junction Solar Cell Efficiencies" Qatar Environment & Energy Research Institute, Doha, Qatar, pp. 0780.

[6] Steiner, M. A., Geisz, J. F., Freidman, D. J., Olavarria, W.J., Duda, A., and Moriarity, T.E., 2011 "Temperature-Dependent Measurements of an Inverted Metamorphic Multijunction (IMM) Solar Cell," 37th IEEE Photovoltaic Specialists Conference (PVSC 37), Seattle, Washington, pp. 4–5.

[7] Mai, C., 2015, "Natural Convection and Radiative Cooling of Concentrated Photovoltaic Cells with Low Profile Heat Sinks," M.S. thesis, Naval Postgraduate School, Monterey, CA.

[8] T.L. Bergman, A. S. Lavine, F. P. Incropera and D. P. Dewitt, 2011, Introduction to Heat Transfer. Hoboken, NJ: John Wiley & Sons.

[9] Massachusetts Institute of Technology, 2016, "19.1 Ideal Radiators," http://web.mit.edu/16.unified/www/FALL/thermodynamics/notes/node134.html.

[10] Diegel, C. R., 2015, "Design and construction of a thermal contact resistance and thermal conductivity measurement system," M.S. thesis, Naval Postgraduate School, Monterey, CA, http://calhoun.nps.edu/handle/10945/47247.

THIS PAGE INTENTIONALLY LEFT BLANK

INITIAL DISTRIBUTION LIST

1. Defense Technical Information Center
   Ft. Belvoir, Virginia

2. Dudley Knox Library
   Naval Postgraduate School
   Monterey, California